Hindawi
Geofluids
Volume 2023, Article ID 1668663, 11 pages
https://doi.org/10.1155/2023/1668663

Research Article

Characterization of Movable Fluid Distribution in Tight Oil Reservoirs by NMR and Centrifugation

Tong Wang[1], **Dongdong Zhang**[1], **Xin Wang**[2], **Zhangchao Wang**[3], **Wen Zhang**[1], **Wenyi Sun**[1], **and Mingyang Ma**[1]

[1]*State Key Laboratory of Continental Dynamics, Department of Geology, Northwest University, Xi'an 710069, China*
[2]*No. 6 Oil Production Plant, Changqing Oilfield Company, PetroChina, Xi'an 710016, China*
[3]*Research Institute of Shaanxi Yanchang Petroleum Group Co., Ltd., Xi'an 710065, China*

Correspondence should be addressed to Dongdong Zhang; zhangdd@nwu.edu.cn

Received 24 May 2022; Revised 24 August 2022; Accepted 25 August 2022; Published 9 February 2023

Academic Editor: Dengke Liu

The reservoir of Chang 7 Member of Yanchang Formation in the Ordos Basin is rich in tight oil resources, with well-developed micro-nanopore throats, strong heterogeneity, and complex fluid distribution characteristics. In this paper, a combination of nuclear magnetic resonance and centrifugation experiments is carried out to qualitatively and quantitatively analyze and evaluate the distribution characteristics of the movable fluid in Chang 7 reservoirs in Baibao Block. With different centrifugal forces, the NMR T_2 spectrum characteristics of saturated water state and different centrifugal force state can be obtained, and the movable fluid distribution characteristics under the control of different centrifugal forces and different pore throat intervals can be obtained. The research results demonstrate that the NMR T_2 spectrum of the Chang 7 tight oil reservoir in the study area presents a double-peak or triple-peak shape. With the increase of centrifugal force, the water saturation value of the corresponding sample gradually decreases. The overall movable fluid saturation ranged from 19.07% to 32.52%, with an average of 26.23% and a low degree of movability. The submicron (0.1~1 μm) and nanoscale (0.075~0.1 μm) pore throats were the main pore throat intervals controlling the movable fluid saturation of the studied samples, accounting for an average of 18.31% and 5.57%, respectively, and micron-scale pore throats ($r > 1\,\mu$m) accounted for an average of 2.35% of the movable fluid distribution.

1. Introduction

In recent years, the global exploration and development of unconventional tight oil and gas has been the focus of scientists' attention [1, 2]. In China, unconventional oil and gas resources such as tight oil, shale gas, and tight gas are now the main source of production growth. Experts and scholars define tight reservoirs as reservoirs with porosity less than 10% and gas permeability less than $1 \times 10^{-3}\,\mu m^2$ [3]. Tight reservoirs are characterized by complex pore structure, micro- and nanoscale pore development, and strong heterogeneity compared with conventional reservoirs, which leads to the complex occurrence and seepage characteristics of fluids in reservoir space [4–7].

The tight oil resources of the Chang 7 member reservoir in the Ordos Basin are very rich, which are controlled by the complexity of micro-nanopore structure [8, 9]. Currently, the flow characteristics of fluid in pore space are not clear, resulting in poor oilfield development effect. NMR experiment is commonly used to characterize the PSD, porosity, permeability, and other rock physical properties of porous media [10, 11]. NMR experiments provide rich information on pore size and the occurrence of fluid. For instance, PSD (pore size distribution), free fluid index as well as bound fluid saturation, and NMR data can even be used to estimate and predict rock physical parameters, such as porosity and permeability in porous media [12–14]. However, NMR in the characterization of fluid distribution in porous media still has many limitations, for example, the distribution characteristics of saturated fluid state of samples can be obtained, and the control effect of different pore throat intervals on movable fluid still needs combing other tests, such as HPMI

(high-pressure mercury injection) and constant-rate mercury injection. In view of the complex petrophysical characterization of the Chang 7 member reservoir, many experts and scholars have conducted qualitative and quantitative studies on its pore structure characteristics and seepage characteristics using NMR techniques, fluid injection techniques, gas adsorption techniques, and some microscopic observation techniques, and the results indicate that the pore throat structure characteristics are the critical factors controlling the differential distribution of movable fluids in this member of the reservoir [15, 16].

In this study, the author combined NMR experiment and centrifugal experiment to characterize the occurrence characteristics of movable fluid in tight oil reservoir. By measuring the NMR T_2 spectrum of the same sample in saturated water state and after different centrifugal forces, different centrifugal forces correspond to different pore throat radius. Therefore, the movable fluid content of samples in different pore throat control intervals can be obtained. Furthermore, the fine evaluation of movable fluid distribution characteristics under the control of tight reservoir pore structure is realized, which provides theoretical support and experimental basis for tight oil and gas development in the future.

2. Geological Background and Samples

The Ordos Basin is located in the central and western regions of China and is the second largest oil and gas bearing basin in the country. It can be further divided into 6 tectonic units according to the internal tectonic features of the basin, in which most of the hydrocarbon resources are distributed within the Yishan Slope tectonic unit [17, 18] (Figure 1). The Mesozoic Late Triassic Yanchang Formation and the Early Jurassic Yan'an Formation are the main oil-bearing systems in the Ordos Basin [19]. The Chang 7 member of the Yanchang Formation is the most widely distributed hydrocarbon source rock within the basin, in which fine-grained sandstone and mud shale are widely developing [20]. Unconventional tight oil and gas resources are abundant, and it is the focus of current exploration and development.

This study takes the tight sandstone reservoir of Chang 7 member in Baibao oilfield as the main research object. The Baibao area is located in the south-central part of the Yishan slope, and the sedimentary facies are dominated by the deep and semideep lacustrine facies, and the lithology is mainly ash black siltstone and fine sandstone [8, 21, 22]. Due to the lack of comprehensive and in-depth understanding of microscopic geological characteristics of Chang 7 member, such as pore and throat structure and occurrence characteristics of fluid, the evaluation of productivity benefit and resource potential of construction, production, and development are limited. Therefore, it is necessary and urgent to explore the characteristics of pore structure and fluid occurrence of Chang 7 member in the study area.

Based on the principle of representativeness and comprehensiveness, five tight sandstone samples from the same layer and different development well sites were obtained from the Baibao oilfield for relevant experimental study and analysis (Table 1). The porosity of the samples was distributed between 6.78% and 10.93%, the average value was 8.51%, the permeability distribution interval was ranged from 0.011 to $0.144 \times 10^{-3}\ \mu m^2$, and the average value was $0.054 \times 10^{-3}\ \mu m^2$. The correlation between porosity and permeability of the studied samples is well, showing overall that samples with higher permeability have higher porosity, with the correlation coefficient R^2 greater than 0.8 (Figure 2).

3. Experiment Method and Procedure

3.1. NNR and Centrifugation. NMR techniques have been are already widely applied to study the distribution of fluids in tight sandstone reservoirs because of their efficiency, nondestructiveness, and accuracy [23, 24]. The main principle is that fluids present in porous media generate detectable signals when subjected to an external magnetic field, and the intensity of the signal is proportional to the number of hydrogen nuclei in the sample [24]. Generally speaking, the larger the pore radius of the sample, the more fluid is present in the pore space, the more fluid can be detected, and the larger the T_2 relaxation time. In other words, the greater the T_2 value, the greater the pore space, vice versa. Therefore, the T_2 distribution obtained from NMR experiments is an objective reflection of the information on the true PSD of the corresponding test sample.

Centrifugal experiments use the centrifugal force of the rock sample centrifuge when rotating at high speed to make part of the fluid in the pore space overcome the capillary pressure resistance, thereby being separated from the sample. By setting different values of centrifugal force, the fluid distribution characteristics under different pore radius control can be obtained. During centrifugation, the relationship between the value of the centrifugal force and the size of the pore radius follows the capillary pressure Equation (1) [25].

$$P_c = \frac{2\sigma \cos\theta}{r}, \tag{1}$$

where $\sigma = 72.5$ mN/m, P_c is the capillary pressure, MPa; θ is the contact angle, the gas-water interface θ is 0°; and r is the radius of the pore throat under the corresponding centrifugal force, μm.

Based on former studies on the fluid distribution characteristics in the tight reservoir of the Chang 7 members using NMR technique, the current study further refines its scheme, and six centrifugal forces of 0.138 MPa, 0.184 MPa, 0.276 MPa, 0.552 MPa, 1.380 MPa, and 1.840 MPa (1 MPa = 145.0326 psi) were set, which roughly correspond to the pore radius of rock samples of 1 μm, 0.75 μm, 0.50 μm, 0.25 μm, 0.10 μm, and 0.075 μm, respectively.

The NMR experimental instrument is the MesoMR23-60H-I NMR experimental instrument produced by Suzhou Niumag analytical instrument corporation, and the model of the centrifuge used is SLJ-10000. The experiment is executed in accordance with the Chinese National Industry Standard SY/T 6490-2014 [26], with the following procedure and steps:

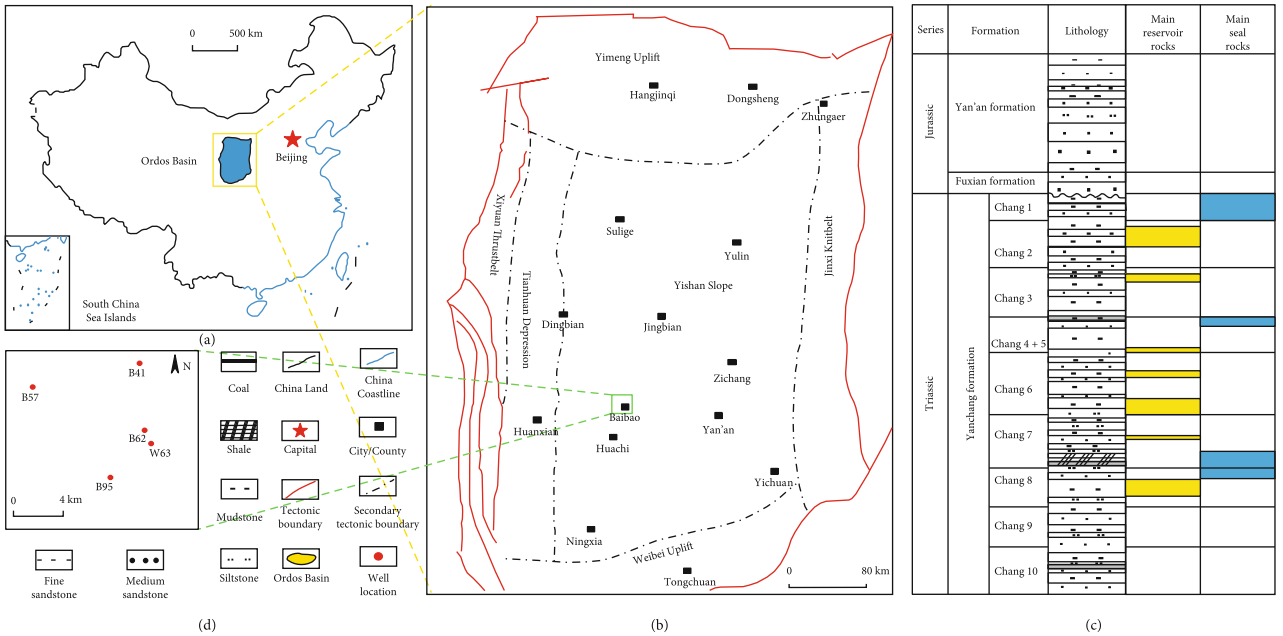

Figure 1: Study area structure and sampling location map (modified from [18]). (a) A map of China. (b) Location map of the study area. (c) The lithology column. (d) Sampling wells' relative location map.

Table 1: Petrophysical characteristics of Chang 7 tight reservoir samples in Baibao oilfield.

Samples	Wells	Depth (m)	Lithology	Length (cm)	Diameter (cm)	Porosity(%)	Permeability ($\times 10^{-3}$ μm^2)
1	B95	2079.09	Fine sandstone	5.016	2.514	7.85	0.018
2	B41	2047.30	Fine sandstone	6.357	2.514	7.36	0.011
4	B62	1944.65	Fine sandstone	4.906	2.514	10.93	0.144
5	B57	2162.00	Fine sandstone	5.721	2.514	6.78	0.026
6	W63	2129.20	Fine sandstone	5.108	2.514	9.65	0.069

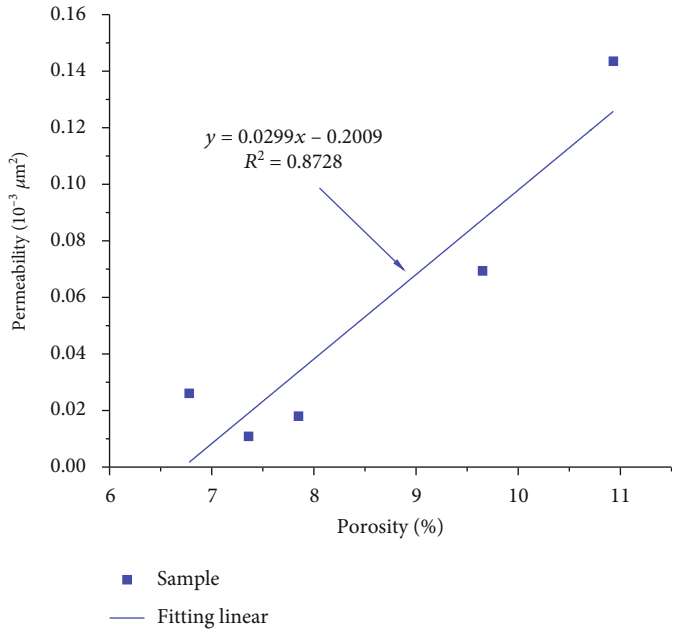

Figure 2: Plots of porosity and permeability correlations for samples from the Chang 7 member of the study area.

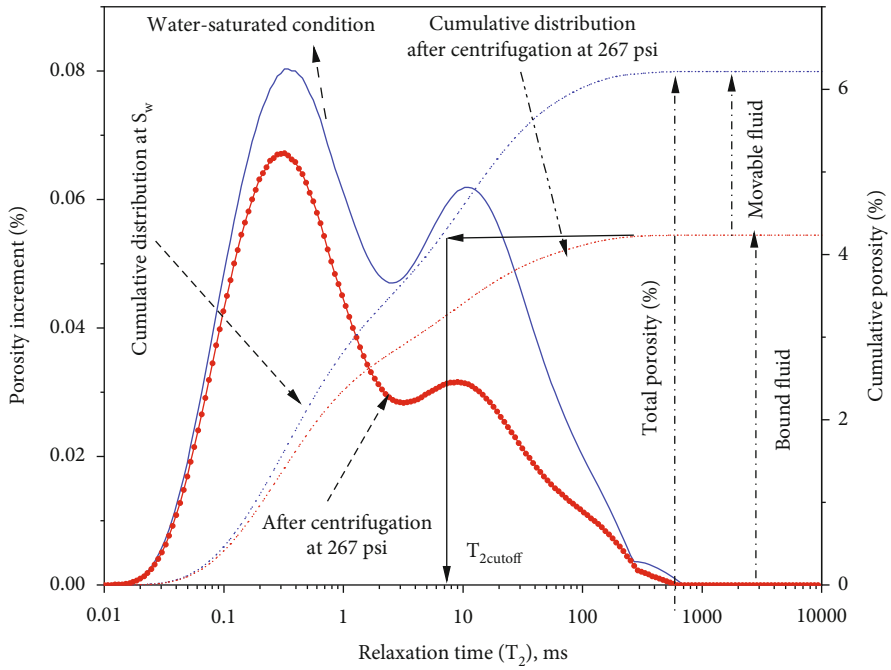

Figure 3: MMR T_2 cutoff value determination method.

(1) The prepared standard cylindrical core samples (length about 40 mm, diameter about 25 mm) were subjected to oil washing operation in order to remove the oil and other impurities remaining in the pore space of the samples, followed by drying the samples in a drying oven at 80°C for 5 hours, weighing their dry weight, length, and diameter, and measuring the porosity and permeability parameters

(2) The dry samples were placed in a vacuum pressurized saturation device and evacuated for 8 h, followed by complete saturation of the experimental samples with simulated formation water for about 24 h at 20 MPa to 25 MPa and weighed. Finally, the samples were wrapped in cling film and placed in the NMR instrument for measurement, after which the T_2 spectral distribution of the corresponding samples was obtained by inversion fitting

(3) After the NMR testing of the samples was completed in the saturated water state, the samples were centrifuged at 20 psi, 27 psi, 40 psi, 80 psi, 200 psi, and 267 psi for a continuous period of 2 h. Following each centrifugation, the samples were subjected to NMR testing to acquire the T_2 spectrum distribution characteristics at different centrifugal force states

3.2. Method of Determining the T_2 Cutoff Value. T_2 cutoff is the key value for calculating the movable fluid parameters of the studied sample. It is generally considered that the fluid in the corresponding small pores with a relaxation time of T_2 less than T_2 cutoff is a bound fluid; otherwise, in the large pores with a relaxation time greater than T_2 cutoff is a free fluid, and this value is a critical value [27].

In the previous studies, scholars usually selected the empirical T_2 cutoff value of the target region as the T_2 cutoff of the study samples. However, due to the strong heterogeneity among Chang 7 tight reservoir samples, sophisticated assembly of pore and throat structure as well as seepage characteristics and T_2 cutoff for the actual samples can be very different from the regional empirical value [9, 28].

In this study, the T_2 cutoff values were determined by measuring the T_2 distribution curves of the samples in the full saturated and centrifuged states, respectively. Taking B62 as an example, the red dashed line is the porosity cumulative distribution of the sample in the saturated water state, and the blue dashed line is the porosity cumulative distribution of the sample in the centrifugal state after the centrifugation at 267 psi. The tangent line of the red dashed line intersects with the blue dashed line, and the T_2 value corresponding to this intersection point is the T_2 cutoff value of this sample [27–29] (Figure 3).

4. Result

4.1. Structural Characteristics of Pore Throat. Through scanning electron microscopy and casting thin section observation statistics of samples from typical wells, results revealed (Figure 4): overall structure of the study samples is quietly tight, with complex pore structure, poor pore development, and diverse types. The main pore types developed are residual intergranular pores, feldspar dissolved pores, intercrystalline pores, and microcrack, with residual intergranular pores and feldspar dissolved pores being the main contributors to the reservoir properties in the study area. In most cases, the feldspathic pores are not developed in isolation and are often connected to the residual intergranular pores (Figure 4(d)),

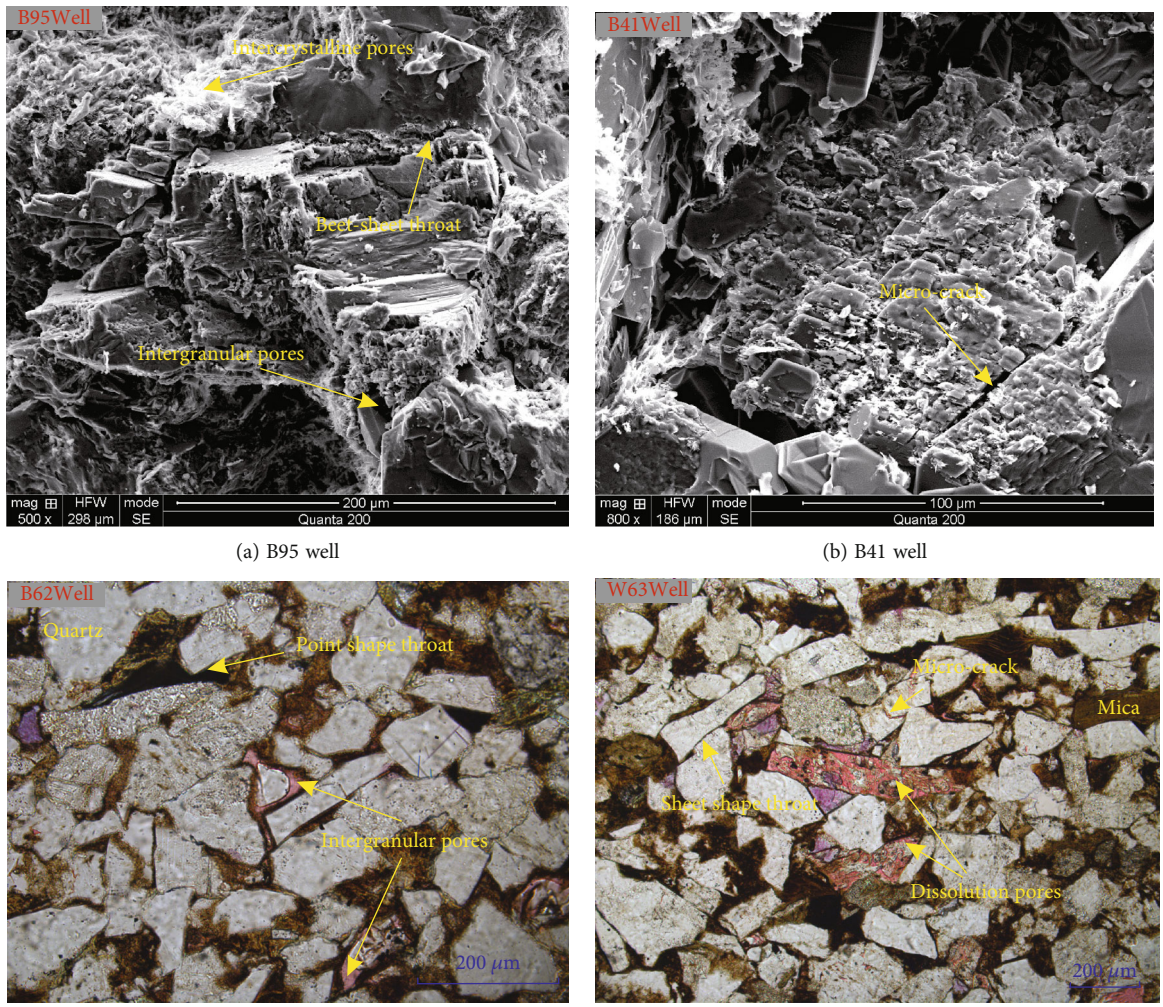

(a) B95 well

(b) B41 well

(c) B62 well

(d) B63 well

Figure 4: The pore and throat characteristics of the samples were studied.

providing good reservoir space for hydrocarbon enrichment, and will largely benefit reservoir physical properties.

For tight reservoirs, the assembly form of the pore throat is a vital factor that controls the mobility of hydrocarbons in the reservoir space. The size and morphology of the throats are strongly related to the size of the rock grains, contact relationships, and later diagenesis. As the samples in the study area have undergone intense late diagenetic compaction, they are mainly characterized by sheet and bent-sheet in SEM and cast thin sections, as well as a small number of points and necking, with the first two types of throat being the most common within the samples studied, showing high numbers and a small radius of the throat (Figure 4).

4.2. NMR T_2 Spectrum. The morphological distribution characteristics of the NMR T2 spectrum are a comprehensive reflection of the rock physical properties such as pore size, number, connectivity, and fluid occurrence characteristics of the rock samples [30, 32]. The T_2 spectrum of cores on the saturated water condition of the Chang 7 member is mostly dominated by bimodal and trimodal morphology, showing an overall higher amplitude of the left peak than the right peak (Figure 5(a)), which indicates that the tiny pores of the Chang 7 member samples are developed, along with a certain amount of large pores, and the connectivity between the pores of different scales is very complicated.

Taking the typical example from B41 well as an example (Figure 5(b)), the T_2 spectrum morphological characteristics of the sample after centrifugation also show the feature of bimodal and trimodal, but the difference is that with the increase of centrifugal force, the NMR pore component signal value decreases continuously, and the magnitude of the right peak decreases more than that of the left peak, which indicates from the side that the movable fluid is mainly stored in the large pores, and some of the movable fluid is driven out by the centrifugal force during the high-speed centrifugation, while the fluid stored in the small pores is difficult or unable to flow due to the capillary binding force.

4.3. Movable Fluid Parameters. The T_2 cutoff values for the 5 samples were calculated separately according to our method mentioned above, which enabled the T_2 cutoff values, movable fluid saturation (Sm), and bound fluid saturation of the corresponding samples to be obtained. The specific

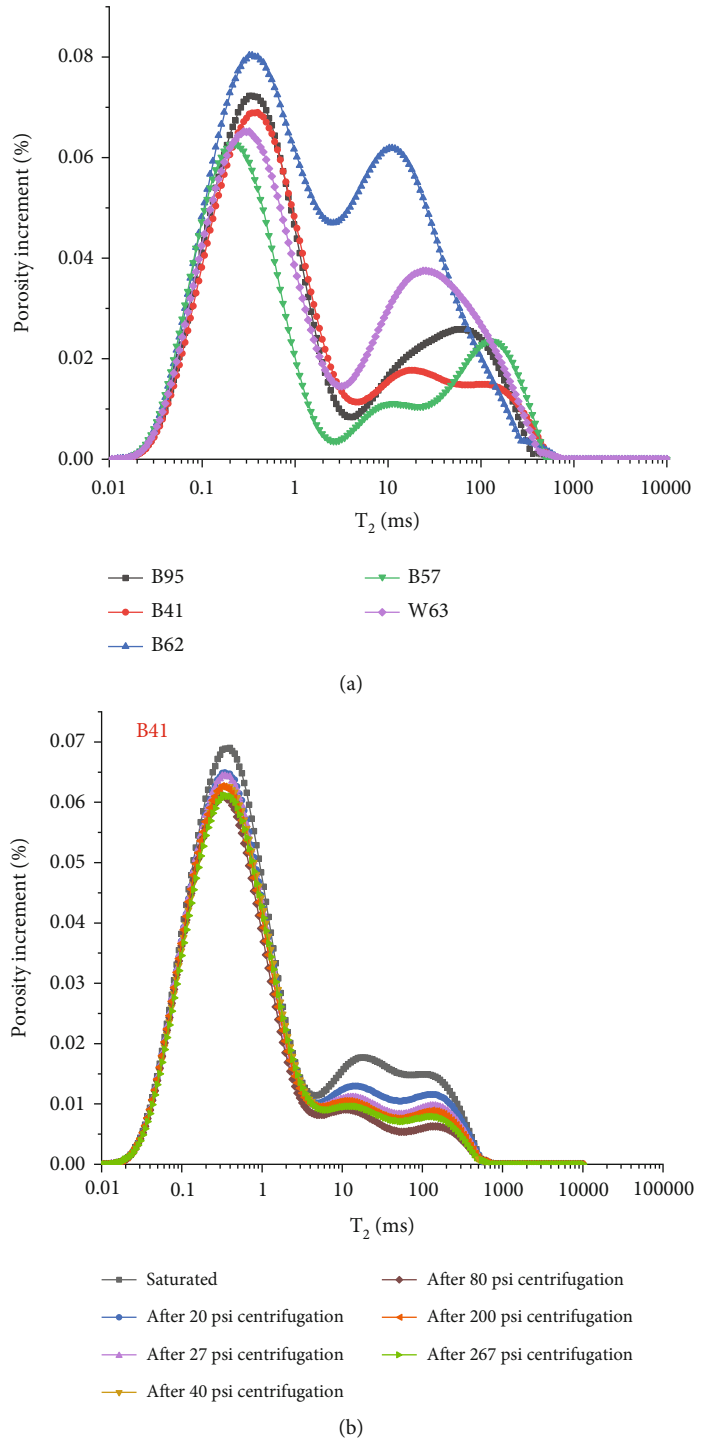

Figure 5: Characteristic of T_2 spectrum in saturated water and centrifugal state: (a) saturated water state. (b) Typical samples in different centrifugal force states.

experimental results are presented in Table 2, where the T_2 cutoff varies greatly between different samples, ranging from 3.92 ms to 18.04 ms, which also indicates that it is not advisable to evaluate the characteristics of movable fluid distribution for variable samples according to the experience value or the T_2 cutoff of the same sample.

For a more visible characterization of the reservoir's movable fluid content, the movable fluid porosity (Φm) parameter is introduced [27, 28, 31], which is numerically $\Phi m = Sm \times \Phi/100$. The Sm of the samples is distributed which varied between 19.07% and 32.52%, with an average of 26.23%. The Φm distribution varied between 1.40% and 3.55%, with an average of 2.29%. Normally, with better sample physical properties, the smaller the T_2 cutoff value and the higher the movable fluid saturation. Taking sample nos. 4, 6, and 5, for example, on the whole, their porosity

Table 2: Distribution characteristics of movable fluid parameters of samples in the Baibao oilfield.

Samples	Porosity (%)	Permeability ($\times 10^{-3}$ μm)	$T_{2cutoff}$ (ms)	Sm (%)	Φm (%)
1	7.85	0.018	3.92	29.15	2.29
2	7.36	0.011	12.75	19.07	1.40
4	10.93	0.144	6.37	32.52	3.55
5	6.78	0.026	18.04	22.96	1.56
6	9.65	0.069	15.70	27.45	2.65

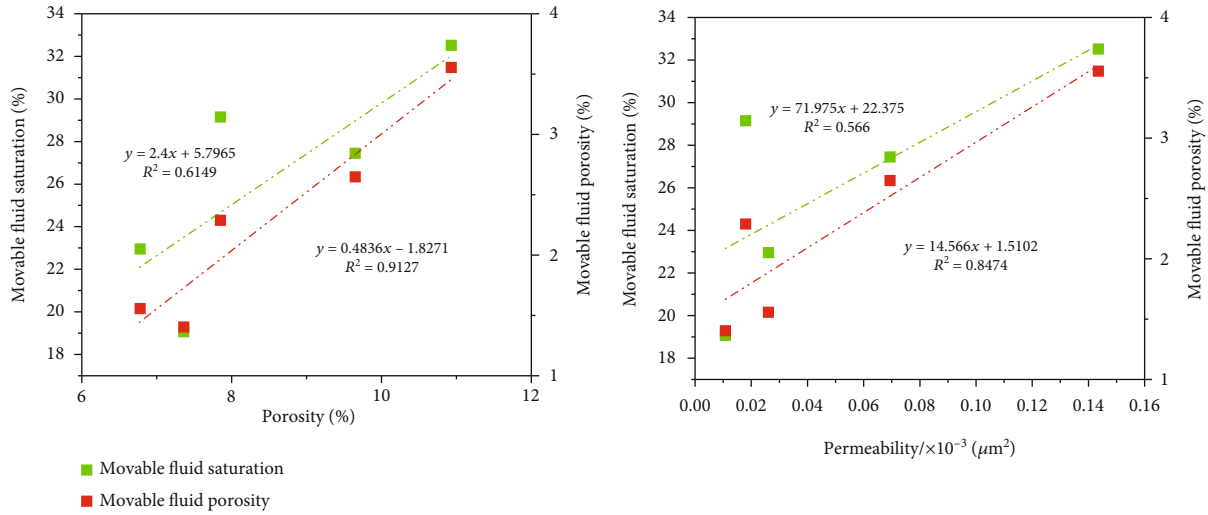

Figure 6: Correlation of movable fluid parameters with their physical properties.

and permeability values decrease successively, T_2 cutoff value gradually increases, and the corresponding movable fluid parameter (Sm and Φm) values also decrease. However, sample 1 is different from the other samples in that the porosity and permeability of sample 1 and sample 2 are very similar, but the difference between their T_2 cutoff value and Sm is very large. The T_2 cutoff value of sample 1 is 3.92 ms while that of sample 2 is 12.75 ms. The difference between the T_2 cutoff values and the movable fluid parameters of these two samples is probably due to the better connectivity between the pore space and the throat of sample 1, which allows fluid to flow easily between the pores and throats, and therefore has a relatively high Sm. By contrast, the pore throat of sample 2 has strong heterogeneity, which will result in a more difficult seepage of the fluid through its pore space, so it has a high T_2 cutoff value and low movable fluid saturation.

5. Discussion

5.1. Relationship between Movable Fluid Content with Physical Parameters. The quality of reservoir physical properties has always been the focus of experts and scholars [32–35]. Physical properties directly determine the basic direction for oilfield development experts to predict favorable reservoir areas. We conducted a correlation analysis between the physical parameters and the movable fluid parameters for the Chang 7 members of the Baibao oilfield. The results show that there appeared a strong positive linear correlation among porosity and permeability with movable fluid parameters, with correlation coefficient R^2 all stronger than 0.56% (Figure 6). Moreover, the correlation between sample physical properties and Φm is greater than that with movable fluid saturation, which illustrates that the application of movable fluid porosity parameters to quantify the content of movable fluids corresponding to reservoir samples is of sufficient scientific significance.

5.2. Distribution Characteristics of Fluid under the Action of Different Centrifugal Forces. The characteristics of the NMR T_2 spectra of the five samples in this experimental study under different centrifugal forces are shown in Figures 5(b) and 7, respectively. With the increase of centrifugal force, the signal values of T_2 spectra all decreased continuously, but the amplitude values of small pores with a T_2 relaxation time less than 5 ms only changed slightly, and the signal values of large pores with a T_2 relaxation time more than 5 ms all decreased significantly with the increase of centrifugal force. This implies that not all movable fluids exist in the large pore spaces and bound fluids in small pore spaces, owing to the complicated structure and poor connectivity of the Chang 7 member pore-throat, which will cause parts of the bound fluids to be trapped in the large "stagnant pore" and parts of the movable fluids stored in the small pore spaces with good connectivity.

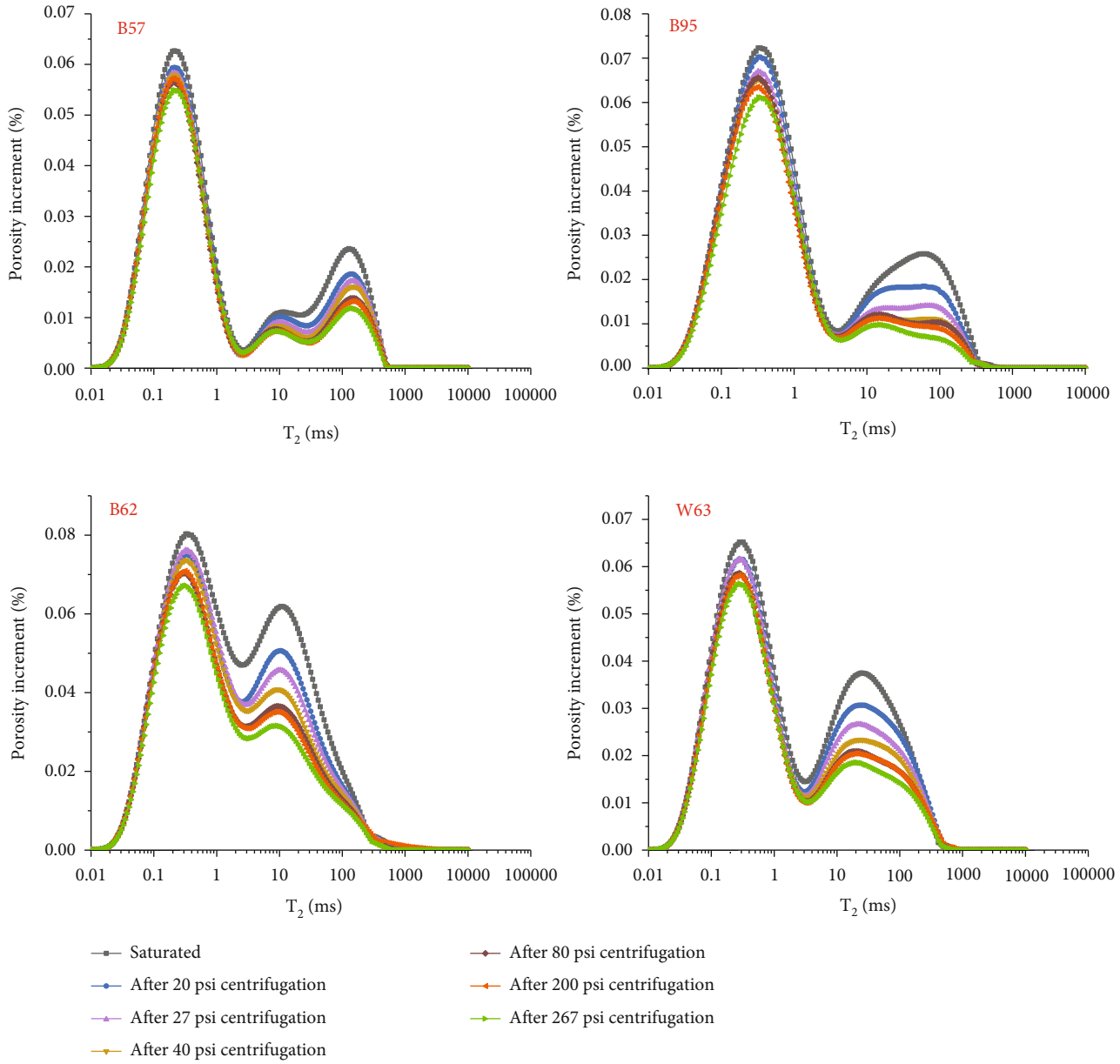

Figure 7: Characteristics of NMR T_2 spectra of samples in the study area after different centrifugal forces.

Figure 8 shows the changes of water saturation of different samples after centrifugal forces of 20 psi, 27 psi, 40 psi, 80 psi, 200 psi, and 267 psi, respectively. It is remarkable that all the five samples have an initial water content saturation of 100%, and the degree of change was greatest in the interval of centrifugal force increase from 20 psi to 80 pai, and when the pressure further goes on continually increasing, the variation of water content saturation decreases.

For example, the water saturation of the W63 well sample (9.65% porosity and $0.069 \times 10^{-3}\ \mu m^2$ permeability) is 91.13% at 20 psi and decreases to 76.99% at 80 psi, at which point most of the movable fluid with a throat radius greater than 0.5 μm has been separated by centrifugal force. When the pressure was increased to 200 psi and 267 psi, the water saturation was 76.41% and 72.36%, respectively, the water saturation changed very little at this time, indicating that most of the movable fluid had been separated, and the residual was immovable water bound by capillary and clay forces.

5.3. Characteristics of Movable Fluid Distribution at Different Throat Radius. The combination of NMR and centrifugation experiments can not only obtain the fluid distribution characteristics at different centrifugal forces but also can obtain the movable fluid saturation under different pore throat controlled intervals [27, 36]. Table 3 makes statistics of movable fluid saturation values controlled by pore throat intervals at different scales of samples in Chang 7 member of the study area under different centrifugal forces. It can be seen that the average values of movable fluid distribution in the range of micrometer ($R > 1\ \mu$m), submicron (0.1-1 μm), and

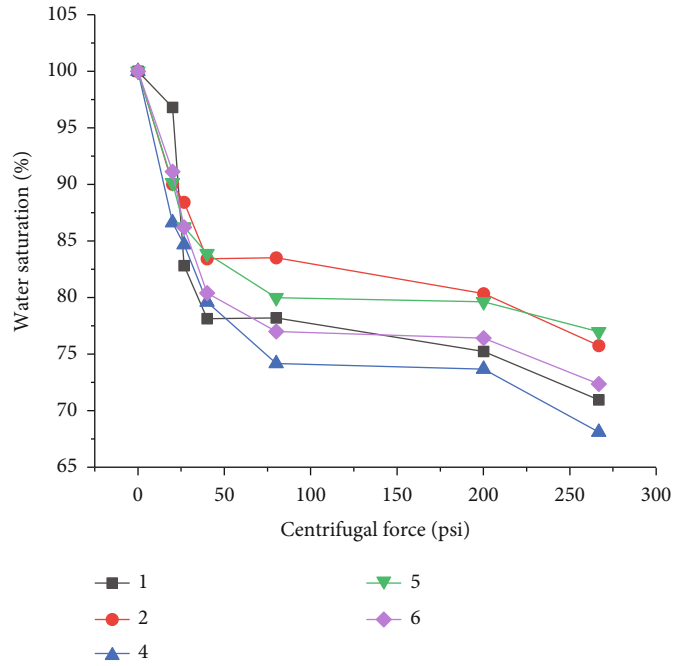

Figure 8: The variation of water saturation of samples under different centrifugal forces.

Table 3: Movable fluid saturation controlled by different pore throat intervals.

Samples	Sm (%)	Sm at different pore throat intervals (μm)					
		0.075~0.1	0.1~0.25	0.25~0.50	0.5~0.75	0.75~1	>1
1	29.15	6.81	5.8	5.11	5.13	4.03	2.27
2	19.07	3.67	3.28	4.37	3.16	2.66	1.93
4	32.52	7.79	6.43	6.31	4.98	3.74	3.27
5	22.96	3.06	3.58	4.46	4.53	5.13	2.20
6	27.45	6.51	5.56	5.42	4.62	3.25	2.09

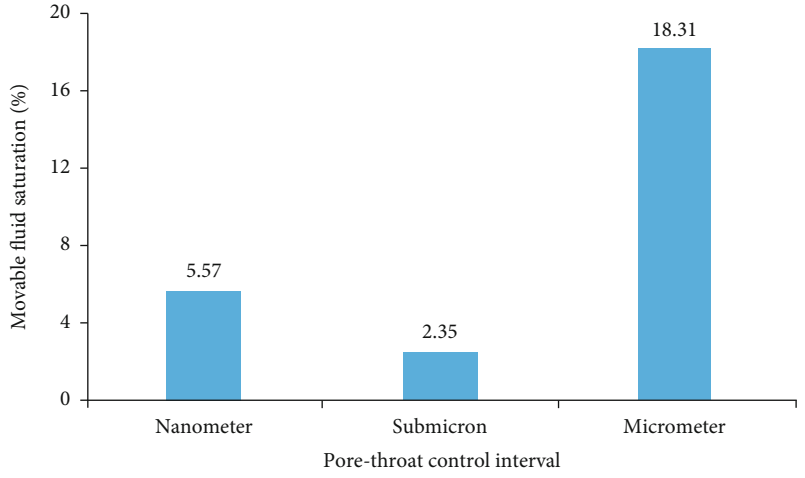

Figure 9: Average movable fluid saturation of samples from the study area at different pore throat control interval.

nanometer (0.075-0.1 μm) are 2.35%, 18.31%, and 5.57% (Figure 9), respectively. A similar rule was also found in the previous study of the content of the movable fluid in the same layer of samples in the adjacent research area [29]. That is, the controlled movable fluid content in the micron, submicron, and nanoscale pore throat intervals is approximated to be 9.01%, 22.55%, and 4.49%. This indicates that the movable fluid in Chang 7 tight reservoir is

mainly controlled by submicron and nanoscale pore throats, which leads to poor fluid seepage ability and low development availability. The content of movable fluid varies greatly among different samples in different pore throat control zones. In general, the movable fluid saturation of Chang 7 member samples in the study area is low, and the content of most movable fluid is controlled by the pore throat space of micro-nano, which is the main reason for the low productivity of Chang 7 member development wells in Baibao area.

6. Conclusions

(1) The NMR T_2 spectrum of the tight oil reservoirs in Chang 7 member of Ordos Baibao oilfield are dominated by bimodal and trimodal, which show that the amplitude of the left peak is higher than that of the right peak, and the amplitude of the right peak decreases more obviously with the increasing centrifugal force, while the left peak does not change much, indicating that most of the movable fluids exist in the connected large pores and the bound fluids exist in the small pores. Owing to the complicated structure of the pore throat, partially bound fluids exist in the large "stagnant pore."

(2) The T_2 cutoff of the samples in Chang 7 of the study area is distributed between 3.92 ms and 18.04 ms, with a wide variation in extremes. The movable fluid saturation distribution ranged from 19.07% to 32.52%, with a mean value of 26.23%, poor reservoir quality, and low mobilization

(3) With the continuous increase of centrifugal force, the movable fluid occurrence in the samples was separated, and the water saturation decreased continuously. The decrease was large before the centrifugal force of 80 psi, but the change was small after the centrifugal force of 80 psi

(4) The content of the movable fluid in the tight reservoir samples of Chang 7 member is dominated by submicron pore throat interval and nanometer pore throat interval, and the corresponding movable fluid content is 18.31% and 5.57%, respectively. The movable fluid content controlled by micron pore throat is the least, which is 2.35%

Data Availability

The data used to support the results of this experiment have been presented in graphical form in the manuscript.

Conflicts of Interest

We declare that there is no conflict of interest in this work.

Acknowledgments

This research was supported by the National Natural Science Foundation of China (no. 41930426).

References

[1] L. Sun, C. Zou, A. Jia et al., "Development characteristics and orientation of tight oil and gas in China," *Petroleum Exploration and Development*, vol. 46, no. 6, pp. 1073–1087, 2019.

[2] W. Zhao, H. Suyun, L. Hou et al., "Types and resource potential of continental shale oil in China and its boundary with tight oil," *Petroleum Exploration and Development*, vol. 47, no. 1, pp. 1–11, 2020.

[3] C. Zou, R. Zhu, K. Liu et al., "Tight gas sandstone reservoirs in China: characteristics and recognition criteria," *Journal of Petroleum Science and Engineering*, vol. 88-89, pp. 82–91, 2012.

[4] D. Ren, D. Zhou, D. Liu, F. Dong, S. Ma, and H. Huang, "Formation mechanism of the Upper Triassic Yanchang Formation tight sandstone reservoir in Ordos Basin–Take Chang 6 reservoir in Jiyuan oil field as an example," *Journal of Petroleum Science and Engineering*, vol. 178, pp. 497–505, 2019.

[5] Y. H. L. S. L. Xianyang, "Characteristics and resource prospects of tight oil and shale oil in Ordos Basin," *Acta Petrolei Sinica*, vol. 34, no. 1, p. 1, 2013.

[6] D. Ren, L. Ma, D. Liu, J. Tao, X. Liu, and R. Zhang, "Control mechanism and parameter simulation of oil-water properties on spontaneous imbibition efficiency of tight sandstone reservoir," *Frontiers in Physics*, vol. 10, no. 10, article 829763, 2022.

[7] D. Ren, H. Zhang, Z. Wang, B. Ge, D. Liu, and R. Zhang, "Experimental study on microscale simulation of oil accumulation in sandstone reservoir," *Frontiers in Physics*, vol. 10, no. 10, article 841989, 2022.

[8] F. Wang, R. Chen, W. Yu et al., "Characteristics of lacustrine deepwater fine-grained lithofacies and source- reservoir combination of tight oil in the triassic Chang 7 member in Ordos Basin, China," *Journal of Petroleum Science and Engineering*, vol. 202, article 108429, 2021.

[9] S. Wu, S. Li, X. Yuan et al., "Fluid mobility evaluation of tight sandstones in Chang 7 member of Yanchang formation, Ordos Basin," *Journal of Earth Science*, vol. 32, no. 4, pp. 850–862, 2021.

[10] C. Lyu, Z. Ning, Q. Wang, and M. Chen, "Application of NMRT2 to pore size distribution and movable fluid distribution in tight sandstones," *Energy & Fuels*, vol. 32, no. 2, pp. 1395–1405, 2018.

[11] J. Li, S. Lu, C. Jiang et al., "Characterization of shale pore size distribution by NMR considering the influence of shale skeleton signals," *Energy & Fuels*, vol. 33, no. 7, pp. 6361–6372, 2019.

[12] F. Benavides, R. Leiderman, A. Souza, G. Carneiro, and R. Bagueira de Vasconcellos Azeredo, "Pore size distribution from NMR and image based methods: a comparative study," *Journal of Petroleum Science and Engineering*, vol. 184, article 106321, 2020.

[13] N. Zhang, S. Wang, F. Zhao, X. Sun, and M. He, "Characterization of the pore structure and fluid movability of coal-measure sedimentary rocks by nuclear magnetic resonance (NMR)," *ACS Omega*, vol. 6, no. 35, pp. 22831–22839, 2021.

[14] H. Wang, Z. Kou, D. A. Bagdonas et al., "Multiscale petrophysical characterization and flow unit classification of the Minnelusa eolian sandstones," *Journal of Hydrology*, vol. 607, article 127466, 2022.

[15] F. Zhang, Z. Jiang, W. Sun et al., "A multiscale comprehensive study on pore structure of tight sandstone reservoir realized by nuclear magnetic resonance, high pressure mercury injection

and constant-rate mercury injection penetration test," *Marine and Petroleum Geology*, vol. 109, pp. 208–222, 2019.

[16] H. Wu, C. Zhang, Y. Ji et al., "An improved method of characterizing the pore structure in tight oil reservoirs: integrated NMR and constant-rate-controlled porosimetry data," *Journal of Petroleum Science and Engineering*, vol. 166, pp. 778–796, 2018.

[17] Y. Yang, W. Li, and L. Ma, "Tectonic and stratigraphic controls of hydrocarbon systems in the Ordos basin: a multicycle cratonic basin in central China," *AAPG Bulletin*, vol. 89, no. 2, pp. 255–269, 2005.

[18] J. Yan, X. He, S. Zhang et al., "Sensitive parameters of NMR T_2 spectrum and their application to pore structure characterization and evaluation in logging profile: a case study from Chang 7 in the Yanchang Formation, Heshui area, Ordos Basin, NW China," *Marine and Petroleum Geology*, vol. 111, pp. 230–239, 2020.

[19] R. Yang, H. Zhiliang, G. Qiu, Z. Jin, D. Sun, and X. Jin, "A Late Triassic gravity flow depositional system in the southern Ordos Basin," *Petroleum Exploration and Development*, vol. 41, no. 6, pp. 724–733, 2014.

[20] F. Jinhua, L. Shixiang, X. Niu, X. Deng, and X. Zhou, "Geological characteristics and exploration of shale oil in Chang 7 Member of Triassic Yanchang Formation, Ordos Basin, NW China," *Petroleum Exploration and Development*, vol. 47, no. 5, pp. 931–945, 2020.

[21] Y. Qu, W. Sun, R. Tao, B. Luo, L. Chen, and D. Ren, "Pore-throat structure and fractal characteristics of tight sandstones in Yanchang Formation, Ordos Basin," *Marine and Petroleum Geology*, vol. 120, article 104573, 2020.

[22] B. Yunlai and M. Yuhu, "Geology of the Chang 7 Member oil shale of the Yanchang Formation of the Ordos Basin in central north China," *Petroleum Geoscience*, vol. 26, no. 2, pp. 355–371, 2020.

[23] B. Wang, X. Zhao, W. Zhou, B. Chang, and H. Xu, "Quantitative characterization of pore connectivity and movable fluid distribution of tight sandstones: a case study of the upper Triassic Chang 7 Member, Yanchang formation in Ordos Basin, China," *Geofluids*, vol. 2020, Article ID 5295490, 13 pages, 2020.

[24] J. Guo, R. Xie, and L. Xiao, "Pore-fluid characterizations and microscopic mechanisms of sedimentary rocks with three-dimensional NMR: tight sandstone as an example," *Journal of Natural Gas Science and Engineering*, vol. 80, article 103392, 2020.

[25] E. W. Washburn, "The dynamics of capillary flow," *Physical Review*, vol. 17, no. 3, pp. 273–283, 1921.

[26] *Subcommittee on Well Logging of Standardization Technical Committee on Petroleum Industry. Standards for Petroleum and Natural Gas Industry:Laboratory Measurement Specification for NMR Parameters of Rock Samples:SY/T 6490-2014*, Petroleum Industry Press, Beijing, 2014.

[27] C. Lyu, Z. Ning, D. R. Cole, Q. Wang, and M. Chen, "Experimental investigation on T_2 cutoffs of tight sandstones: comparisons between outcrop and reservoir cores," *Journal of Petroleum Science and Engineering*, vol. 191, article 107184, 2020.

[28] Q. Zang, C. Liu, R. S. Awan et al., "Occurrence characteristics of the movable fluid in heterogeneous sandstone reservoir based on fractal analysis of NMR data: a case study of the Chang 7 Member of Ansai Block, Ordos Basin, China," *Journal of Petroleum Science and Engineering*, vol. 214, article 110499, 2022.

[29] P. Li, C. Jia, Z. Jin, Q. Liu, M. Zheng, and Z. Huang, "The characteristics of movable fluid in the Triassic lacustrine tight oil reservoir: a case study of the Chang 7 member of Xin'anbian Block, Ordos Basin, China," *Marine and Petroleum Geology*, vol. 102, pp. 126–137, 2019.

[30] X. Liu, Z. Jin, J. Lai et al., "Fractal behaviors of NMR saturated and centrifugal T2 spectra in oil shale reservoirs: the Paleogene Funing formation in Subei basin, China," *Marine and Petroleum Geology*, vol. 129, article 105069, 2021.

[31] H. Gao and H. Li, "Determination of movable fluid percentage and movable fluid porosity in ultra-low permeability sandstone using nuclear magnetic resonance (NMR) technique," *Journal of Petroleum Science and Engineering*, vol. 133, pp. 258–267, 2015.

[32] H. Huang, W. Sun, W. Ji et al., "Effects of pore-throat structure on gas permeability in the tight sandstone reservoirs of the Upper Triassic Yanchang formation in the Western Ordos Basin, China," *Journal of Petroleum Science and Engineering*, vol. 162, pp. 602–616, 2018.

[33] J. Wang, S. Wu, Q. Li, J. Zhang, and Q. Guo, "Characterization of the pore-throat size of tight oil reservoirs and its control on reservoir physical properties: a case study of the Triassic tight sandstone of the sediment gravity flow in the Ordos Basin, China," *Journal of Petroleum Science and Engineering*, vol. 186, article 106701, 2020.

[34] G. Sheng, Y. Su, and W. Wang, "A new fractal approach for describing induced-fracture porosity/permeability/compressibility in stimulated unconventional reservoirs," *Journal of Petroleum Science and Engineering*, vol. 179, pp. 855–866, 2019.

[35] M. Liang, F. Guang, X. Han, and Q. Li, "Mapping of oil-source faults in reservoir-cap rock combinations without a source rock," *Energy Geoscience*, vol. 3, no. 2, pp. 103–110, 2022.

[36] F. Dong, X. Lu, Y. Cao, X. Rao, and Z. Sun, "Microscale pore throat differentiation and its influence on the distribution of movable fluid in tight sandstone reservoirs," *Geofluids*, vol. 2021, Article ID 6654773, 7 pages, 2021.

[37] P. Li, W. Sun, B. Wu, Y. Gao, and K. Du, "Occurrence characteristics and influential factors of movable fluids in pores with different structures of Chang 63 reservoir, Huaqing Oilfield, Ordos Basin, China," *Marine and Petroleum Geology*, vol. 97, pp. 480–492, 2018.